
AUTO-VECTORIZING TENSORFLOW GRAPHS: JACOBIANS, AUTO-BATCHING AND BEYOND

Ashish Agarwal¹ Igor Ganchev¹

ABSTRACT

We propose a static loop vectorization optimization on top of high level dataflow IR used by frameworks like TensorFlow. A new statically vectorized parallel-for abstraction is provided on top of TensorFlow, and used for applications ranging from auto-batching and per-example gradients, to jacobian computation, optimized map functions and input pipeline optimization. We report huge speedups compared to both loop based implementations, as well as run-time batching adopted by the DyNet framework.

1 INTRODUCTION

Today’s machine learning applications operate on huge multi-dimensional arrays, or *tensors*, and typically run algorithms involving large chunks of parallelizable computations. The inherent vectorization opportunities are typically leveraged by writing highly optimized libraries of common operations, or *kernels*, for each platform. Common frameworks like TensorFlow (Abadi et al., 2016) and PyTorch (Paszke et al., 2017) contain hundreds of such kernels, which can be viewed as the instruction set for writing ML programs. Using this instruction set of kernels, and optionally other control flow constructs, most frameworks define a high level *IR* (intermediate representation) which is either constructed explicitly, or implicitly via tracing JIT (e.g. (Frostig et al., 2018)). This IR either gets interpreted, or JIT or AOT compiled after going through different layers of optimizations. (The XLA team, 2017; Wei et al., 2017; Chen et al., 2018).

We propose a static loop vectorization optimization that operates on this high level IR. In contrast to CPU instruction sets, these kernels often allow fusing arbitrary number of scalar instructions, where the count may not even be known statically. Thus instead of statically unrolling a fixed number of loop iterations, one can conceptually unroll the full loop and fuse the contained instructions, often completely getting rid of the loop, especially for embarrassingly parallel computation. This process can then be repeated in cases with nested control flow constructs.

We have implemented a library that performs vectorization

¹Google Inc, Mountain View, California, USA. Correspondence to: Ashish Agarwal <agarwal@google.com>, Igor Ganchev <iga@google.com>.

on TensorFlow Graph IR. The optimization triggers during the graph construction phase and can currently vectorize more than a hundred different types of kernels. The user provides the body of a parallel-for loop and gets back symbolic tensors representing the result of a vectorized version of that loop.

This construct of vectorization-optimized parallel-for loop lends itself to many interesting applications. A commonly desired use case is auto-batching (Looks et al., 2017; Neubig et al., 2017) wherein the user writes model code on a single example and then applies that function to each input in a batch. Such code is more intuitive and simpler, especially for models involving dynamic computation graphs. Auto-batching can be implemented by putting the forward pass of the model inside a parallel-for loop with batch size number of iterations. A variant of this is getting per-example gradients, which can be computed by putting both the inference and the gradient computation inside a parallel-for loop. Increasingly, models involve more deeply nested sequential and parallel loops, like iteration over sequence inputs (Gers et al., 2000), Markov Decision Processes, sampling or particle filters for stochastic models, adaptive computation (Graves, 2016), and many more, providing a huge opportunity for applying these techniques.

Another commonly desired application is computing *jacobians*. When the output of a network is a vector or tensor, jacobian involves computing gradients of each scalar value in the output. This is a powerful mathematical object but unfortunately not supported natively by TensorFlow which implements jacobian-vector products instead. Iterative approaches often end up being slow. Putting gradient computation of each output element in a parallel-for loop and vectorizing it enables more efficient computation. Additionally it enables many cases that don’t currently work in TensorFlow, like jacobians of dynamic RNNs or *hessians*

of non-scalar outputs. Our jacobian implementation has enabled new research work like (Pfau et al., 2018) and (Matt Golub, 2018).

2 RELATED WORK

Auto vectorization is a well known technique applied by compilers like GCC and LLVM and has been well researched in literature. (Nuzman et al., 2006) proposed compiler transformations that support vectorization in the presence of interleaved data. A polyhedral model (Trifunovic et al., 2009) can be used to estimate the performance impact of the different loop transformations and vectorization strategies. (Barik et al., 2010) use dynamic programming for selecting vector instructions. Techniques for performing whole function vectorization is discussed in (Karrenberg & Hack, 2011). *ispc* (Pharr & Mark, 2012) proposed an SPMD programming model for graphics workload. Halide (Ragan-Kelley et al., 2013) provides a model for separation of algorithm from schedule, allowing stochastic search over space of schedules.

Most of these approaches operate at much lower level of abstraction and hence miss out on domain specific optimizations, like leveraging linear algebra identities. Frameworks like TensorFlow XLA (The XLA team, 2017), TVM (Chen et al., 2018) and DLVM (Wei et al., 2017) follow a staged compilation approach, and can fuse operations at high level. Our work operates at a similar or higher abstraction level and proposes applying loop vectorization along with adding a new parallel-for user abstraction.

Auto-batching is a special case of vectorization and has been used by TensorFlow Fold (Looks et al., 2017) and DyNet (Neubig et al., 2017). Both these approaches use run-time or *dynamic batching*, which is very flexible and can work even when the kernels are dispatched dynamically from a host language like Python. However dynamic batching can potentially incur large overheads, both in trying to identify and fuse operations, as well as in collating the inputs and slicing the outputs when necessary. Additionally control flow dependent on computation can cause the dispatch to stall and hence fusion cannot work across it.

A static auto vectorization approach can reduce the dispatch overheads, vectorize across nested control flow and allow additional post-vectorization optimizations. In dynamic environments, the technique could be applied to JIT compiled traces (Frostig et al., 2018). We recently became aware of static auto-batching effort (Salesforce, 2018) for PyTorch which works by rewriting the Python AST. We believe that static analysis on Python could potentially miss out on optimization opportunities given that types may not be known statically, or it would have to delay it to run-time which may incur additional overheads. By performing static auto

vectorization on strongly typed high level IR, we are able to achieve large speedups across a range of applications.

3 COMPILATION DETAILS

3.1 Programming Model

We assume a dataflow programming model, extended to handle state and control flow, similar to the one used for TensorFlow (Yu et al., 2018). A directed cyclic graph represents a program or computation. Its nodes represent *operations*, or primitive functions. Its edges represent data flowing between operations. Edges incident into a node represent its inputs, and edges incident out of the node represent its outputs. Both inputs and outputs are ordered. The data on edges can be either immutable *tensors* or mutable *variables*. Both tensors and variables are multi-dimensional arrays of primitive types.

Nodes get ready to run when all their inputs are ready. When multiple nodes are ready, they can be executed in any order or in parallel. Besides the edges representing data dependencies, the model includes edges representing *control dependencies*. A control edge from node η_1 to node η_2 enforces that node η_2 is executed after node η_1 .

The graph can have cycles due to loops and may have special operation nodes to implement different control flow semantics. In addition, we assume that all operation types as well as the types of all input and output tensors are known at compile time. Full or partial shapes may be known statically as well.

Even though we focus on a dataflow based programming model, for the purpose of exposition, we will write imperative pseudocode and examples. These snippets should be seen as building the dataflow graph. For example $Z = \text{matmul}(X, Y)$ represents a subgraph with a single node representing the operation *matmul* with two input edges, X and Y , and a single output edge Z . Similarly, imperative constructs like *for*, *while*, *if-then-else* should be seen as constructing the corresponding control flow constructs in the graph. In addition, we will use *parfor* to represent a *parallel-for* loop. Its semantics will be discussed in more detail in §3.3.

3.2 Notation

We use the following notation. γ represents program segments, corresponding to subgraphs in the overall dataflow graph. Optionally, we use notation $\gamma(\text{args})$ to identify the set *args* as some of the inputs of interest to γ . $\hat{\gamma}$ represents the compiled version of γ , where the goal and semantics of compilation will be described in subsequent sections. η will represent a node in γ and $\hat{\eta}$ is its compiled version in $\hat{\gamma}$. It may be a single node or a sub-graph. op_η is the op-

eration for the node η . For any X which is a tensor (or a sequence of tensors), \hat{X} represents the *vectorized* version of X . A vectorized version means that \hat{X} stores n different versions of X in some layout. X_j , where j is an integer, or a vector of integers, refers to a row (or rows) j along the first dimension and either *gathers* them into a new tensor, or references them as a mutable variable. If X is a sequence, the definition applies recursively for each element. However if \hat{X} represents a vectorized version of X , then \hat{X}_j represents the j^{th} version of X , if j is scalar. If j is a vector, \hat{X}_j represents a vectorized entity that *subsets* the underlying versions to be j , i.e. only includes versions j .

3.3 Problem Statement

Given a dataflow graph Γ represented by the parallel-for loop of the form

```

parfor  $i = 0$  to  $n - 1$  do
     $\gamma(i)$ 
end for
    
```

where n is a scalar integer tensor whose value may only be known at run-time, and $\gamma(i)$ is a set of instructions that may depend on the loop variable i , as well as any global state, the goal of the compilation process is to generate a new dataflow graph, $\hat{\gamma}(n)$, that is functionally equivalent to Γ , and that tries to get rid of or reduce the scope of the `parfor` loop.

A `parfor` loop is defined similar to a `for` loop with the difference that the iterations don't need to run in sequential order. Instead the output and side-effects of the execution should be the same as under a *SIMD* execution model.

A SIMD execution of Γ involves dispatching the nodes of $\gamma(i)$ in lock step for all `active` iterations, which are the iterations of the loop that are executing that operation. This set starts off as being $\{0, \dots, n - 1\}$. Whenever a control flow block construct is encountered, the set is updated to be the set of iterations that continue execution of that block and other inactive iterations stall, waiting for the block to finish. For `parfor`, note that we don't require that the instructions actually be run in lock-step across all active iterations, but that the global state when the execution is done be the same as after a SIMD execution.

3.4 Compiling Stateless Operations

We start with the case where the result of `parfor` is the same under any ordering or interleaving of the execution of the different iterations. (i.e. no data dependencies between any of the iterations, and no side-effects). §3.8 will describe adding support for stateful operations.

Here we provide examples on how to compile simple stateless graphs, building towards our conversion algorithm in

§3.5. We will directly list $\gamma(i)$ in our examples below and assume that it is wrapped in a `parfor` as illustrated in §3.3. $\hat{\gamma}$ will be the vectorized version and the last expression will be assumed to be the returned value. Shapes of the inputs are listed on the first line.

An important aspect demonstrated here is how we leverage `loop invariance` of tensors beyond what traditional approaches to loop invariant code motion achieve. This will involve generating different code based on what combinations of input values are loop invariant.

For the purpose of examples here and later, we adopt the following layout for vectorized tensors. We assume here that shapes are fixed across iterations. Let X have shape $[s_0, \dots, s_r]$. Then we can layout \hat{X}_j by stacking all the versions of X sequentially. Given that, shape of \hat{X} is $[n, s_0, \dots, s_r]$ and $\hat{X}_j = \hat{X}[j], 0 \leq j < n$, corresponds to the value of X in iteration j . However if X is loop invariant, \hat{X} has same shape as X and represents the value of X in all iterations, i.e. we avoid unnecessary stacking. For cases where shape of X is different across iterations, more complicated book-keeping is needed, and we ignore such cases for the examples here. Also note that when shape information is statically available it can be used for more efficient code generation. Else the compiler generates code conditioned on run time shapes.

The common operation of gathering the i^{th} row of a tensor with first dimension n can be vectorized as follows.

```

input  $X : [n, x]$ 
     $\gamma(i) : X[i]$ 
     $\hat{\gamma}(n) : X$ 
    
```

In the more general case, gathering rows can be vectorized as a slicing operation on X .

```

input  $X : [m, x]$ 
     $\gamma(i) : X[i]$ 
     $\hat{\gamma}(n) : X[0 : n, \dots]$ 
    
```

Component-wise operations can invoke the original operation.

```

input  $X : [n, x, y], Y : [n, x, y]$ 
     $\gamma(i) : X[i] + Y[i]$ 
     $\hat{\gamma}(n) : X + Y$ 
    
```

Typically such operations support broadcasting ([The SciPy community, 2008](#)) that semantically tiles the inputs along corresponding dimensions to get the shapes to match before component-wise operations are performed. Shapes are left extended with 1 to get ranks to match, and corresponding dimensions should have equal values or at least one of them should be 1.

Compilation may need extra reshapes to makes sure broad-

casting works for generated code. Also note below how it handles loop invariant input X and gets away without having to tile it n times. Here *reshape* is assumed to reshape the input without copying the underlying data.

input $X : [y, z], Y : [n, z]$
 $\gamma(i) : X + Y[i]$
 $\hat{\gamma}(n) :$
 $X1 = \text{reshape}(X, [1, y, z])$
 $Y1 = \text{reshape}(Y, [n, 1, z])$
 $X1 + Y1$

Now assume *matmul* performs matrix multiplication and *batch_matmul* takes two lists of matrices (as 3-D tensors) and performs matrix multiplication on the corresponding values in the lists.

input $X : [n, x, y], Y : [n, y, z]$
 $\gamma(i) : \text{matmul}(X[i], Y[i])$
 $\hat{\gamma}(n) : \text{batch_matmul}(X, Y)$

The above is effectively the same as the uncompiled version. However if one of the inputs is loop invariant, this can be optimized based on the mathematical properties of matrix multiplication.

input $X : [n, x, y], Y : [y, z]$
 $\gamma(i) : \text{matmul}(X[i], Y)$
 $\hat{\gamma}(n) :$
 $X1 = \text{reshape}(X, [n * x, y])$
 $R = \text{matmul}(X1, Y)$
 $\text{reshape}(R, [n, x, z])$

Next assume *conv2D* performs convolution on the input using the passed in filter. We will assume that the operation performs padding of the input to ensure that the output shape for each channel is the same as input.

input $X : [n, b, h, w, c1], F : [k1, k2, c1, c2]$
 $\gamma(i) : \text{conv2D}(X[i], F)$
 $\hat{\gamma}(n) :$
 $X1 = \text{reshape}(X, [n * b, h, w, c1])$
 $R = \text{conv2D}(X1, F)$
 $\text{reshape}(R, [n, b, h, w, c2])$

Next we look at reductions. Here *reduce_sum* reduces the input by performing sum reduction along the passed in axes. The generated code renumbers the axes and calls the same reduction.

input $X : [n, x, y, z]$
 $\gamma(i) : \text{reduce_sum}(X[i], [1, -1])$
 $\hat{\gamma}(n) : \text{reduce_sum}(X, [2, -1])$

Renumbering of axes works for a lot of other operations. Here is an example of *concat* which concatenates a list of tensors along a particular axis.

input $X : [n, x, z], Y : [n, y, z]$

$\gamma(i) : \text{concat}((X[i], Y[i]), 1)$
 $\hat{\gamma}(n) : \text{concat}((X, Y), 2)$

In our implementation described in §4, we added support for converting more than 100 different operations. As illustrated by above examples, lot of these conversions involve calling the original operation op_η with additional reshape and occasional transposes. In other cases, op_η is flexible in the length of one dimension, often a *batch* and sometimes a *channel* dimension, and operates independently on each slice along that dimension. In such cases, one could fold the first dimension of \hat{X} into the that dimension, run op_η , and transpose and reshape the outputs back as needed. Renumbering axes was another common approach.

Note that whether a particular input is loop invariant or not is independent of the operation being converted and is a property of how the dataflow graph was structured. Hence when implementing a converter, one may need to consider all possible combinations of loop invariance of its inputs. However based on typical graphs compiled, and based on which of those combinations can be expressed efficiently using the set of operations available to the framework, one can leave most of these combinations unoptimized by falling back to the loop based implementation as written above. This fallback provides a path for incrementally baking in more optimizations over time.

3.5 Greedy Algorithm

We provide a greedy algorithm for the problem stated in §3.3. Given the dataflow graph corresponding to $\gamma(i)$, we first convert it to a directed acyclic graph by converting each control flow block into a single node. Next we traverse this new dataflow graph in topological order, and for each node η , generate a new set of nodes, $\hat{\eta}$, that efficiently implement the functionality of running η in a `parfor`. Any control dependencies of η are mirrored for each node in $\hat{\eta}$. Each output tensor X of η is mapped to a new tensor (or sequence of tensors) \hat{X} in $\hat{\eta}$ that stores all the versions of X across all iterations using some chosen layout.

Code generation is done by using a registry of *converters* keyed by the signature of the operation, op_η corresponding to the node η . See §3.4 and §3.8 for discussion on these converters. If the node represents a control flow block in the original graph, special logic is employed which traverses the nodes corresponding to this block, strips out control flow operations and extracts sub graphs that correspond to semantics blocks of that control flow, like the `body` and `condition` of loops, or the `condition`, `then` and `else` blocks for conditionals, etc. These blocks are recursively converted and new control flow code is generated as detailed in §3.6 and §3.7.

3.6 Compiling Conditionals

Next we look at compiling code with conditionals. Consider the code segment below where T and R are tensors or sets of tensors, and γ^{pre} , γ^{cond} , γ^{then} and γ^{else} are code segments representing dataflow subgraphs.

```

parfor  $i \leftarrow 0$  to  $n - 1$  do
   $T, C \leftarrow \gamma^{pre}(i)$ 
  if  $C$  then
     $R \leftarrow \gamma^{then}(i, T)$ 
  else
     $R \leftarrow \gamma^{else}(i, T)$ 
  end if
end for
    
```

Below is a functionally equivalent code segment that gets rid of the `parfor`. The idea is to evaluate the `if` condition for all the iterations, then compute the indices of the iterations, I^{then} and I^{else} , that would go into the `then` and `else` blocks respectively. Given these indices, we compile γ^{then} and γ^{else} to work for only those particular iterations. The compilation process needs to care about some details. Firstly, it needs to subset any vectorized tensors to only those active indices. Secondly any references to i in γ^{then} should vectorize to I^{then} (similarly I^{else} for γ^{else}). Also, the number of iterations should be set to be n^{then} and n^{else} respectively. Given these things are taken care of, the converter for conditionals can call the compilation module recursively to convert γ^{then} and γ^{else} .

```

 $\hat{T}, \hat{C} \leftarrow \hat{\gamma}^{pre}(n)$ 
 $I^{then} \leftarrow \{j : \hat{C}_j \text{ is True}\}$ 
 $n^{then} = \text{length}(I^{then})$ 
 $I^{else} \leftarrow \{j : \hat{C}_j \text{ is False}\}$ 
 $n^{else} = \text{length}(I^{else})$ 
if  $n^{then} > 0$  then
   $\hat{T}^{then} \leftarrow \hat{T}_{I^{then}}$ 
   $R^{then} \leftarrow \hat{\gamma}^{then}(n^{then}, \hat{T}^{then})$ 
end if
if  $n^{else} > 0$  then
   $\hat{T}^{else} \leftarrow \hat{T}_{I^{else}}$ 
   $R^{else} \leftarrow \hat{\gamma}^{else}(n^{else}, \hat{T}^{else})$ 
end if
 $\hat{R} \leftarrow \text{Scatter}((I^{then}, I^{else}), (R^{then}, R^{else}))$ 
    
```

where `Scatter` stitches back the partial results from the two branches based on the indices that each branch processed. An interesting case is when loop condition C is loop invariant. In such cases, the subsetting operations can be skipped for performance reasons.

3.7 Compiling Nested Loops

Now let us consider the case of loops nested inside the `parfor`. If that loop is itself a `parfor` loop, then the compiler can be invoked to convert it first. In case of se-

quential `while` and `for` loops, corresponding converters need to be invoked. If these loops are deeply nested, each converter will in turn invoke compilation recursively which will lead to converting these loops inside out.

Here is a `while` loop nested inside a `parfor`. As before T and R are tensors or sets of tensors, and γ^{pre} , γ^{cond} and γ^{body} are code segments representing dataflow subgraphs.

```

parfor  $i \leftarrow 0$  to  $n - 1$  do
   $R, T \leftarrow \gamma^{pre}(i)$ 
  while  $\gamma^{cond}(i, R, T)$  do
     $R \leftarrow \gamma^{body}(i, R, T)$ 
  end while
end for
    
```

Below is the functionally equivalent code that gets rid of the `parfor`. The overall idea is to generate another `while` loop where, in each iteration, we keep track of the indices, I , of all `parfor` loops that are still active, and run the condition and body, $\hat{\gamma}^{cond}$ and $\hat{\gamma}^{body}$, on only those indices. Similar to the conditional case, this involves subsetting all the vectorized inputs of those blocks to the set I , and having the recursive compilation be aware of the list and count of active iterations. Also, a more optimized implementation can be done for the case where the output of γ^{cond} is loop invariant.

```

 $\hat{R}, \hat{T} \leftarrow \hat{\gamma}^{pre}(n)$ 
 $done \leftarrow false$ 
 $I \leftarrow [0, \dots, n - 1]$ 
 $l \leftarrow n$ 
while not  $done$  do
   $C \leftarrow \hat{\gamma}^{cond}(l, R_I, \hat{T}_I)$ 
   $I' \leftarrow \{j : C_j \text{ is true}\}$ 
   $I \leftarrow I'$ 
   $l \leftarrow \text{length}(I)$ 
  if  $l$  is 0 then
     $done \leftarrow true$ 
  else
     $R_I \leftarrow \hat{\gamma}^{body}(l, R_I, \hat{T}_I)$ 
  end if
end while
    
```

3.8 Compiling Stateful Operations

Most of discussion till now has ignored stateful operations. Turns out even handling stateless operations is sufficient for optimizing many practical applications. Nonetheless we extend our approach for stateful operations.

For cases where $\hat{\eta}$ touches (reads or writes) any mutable state, we adopt the following safety mechanism. Firstly, any accesses to state start only after all the inputs are ready. Secondly, all state accessed anywhere by $\hat{\eta}$ is protected (using mutex) for the entire duration of any state accesses. Lastly, the first output should be produced only after all accesses

to state are done. This allows us to simulate a similar ordering imposed when executing η . See §3.9 for how this assumption helps prove equivalence of the converted code.

Operations that mutate state may often not be SIMD compatible. Even assigning a value to a mutable variable is not compatible, unless the value assigned is loop invariant. Given that a user is putting this call in a `parfor` loop, there are multiple options to handle it. Firstly, it could be raised as an error. Secondly, assuming these calls are intended and useful, they could be overloaded with special semantics. Thirdly, if instead of SIMD semantics, user intended sequential semantics, the conversion could be implemented for sequential output. Choice of these options could be driven by context (e.g. we were optimizing a sequential loop vs parallel loop) as well as special flags (raise error vs overload semantics for SIMD case).

An example of such a case is random number generation. The call is not SIMD compatible since each call involves reading and updating some internal mutable state. However in SIMD setting it could be desirable to change the shape passed to the generator, increasing the rank by 1. Note that the output may or may not be the same as under sequential semantics based on the implementation of the generator.

We now discuss some common cases of stateful converters. First we consider operations that are idempotent. Typical examples include get-or-create a named mutable tensor or reading the value of a mutable tensor. Given the idempotent nature these can be run once and the outputs can be marked as loop-invariant. Next we consider operations that are commutative and associative. Examples include adding or subtracting a value into a mutable tensor. Efficient implementation for such operations is done by first reducing all the updates and then applying the reduced value to the mutable state.

3.9 Discussion

Greedy conversion can miss out on many optimization opportunities. For example, data layout used when converting a node could be better chosen based on the nodes consuming the output. Operations generated for one node could be potentially fused or swapped with subsequently generated ones. Some of these optimizations can be done independently in subsequent rewrite passes.

Vectorization can have trade-offs. Memory utilization is typically larger and memory constraints may inhibit conversion. Vectorization may not even speed up the compute. Additional cost models, heuristics and search may be needed to figure out when and how much to vectorize. However given that we expect a staged compilation, we contend that downstream optimizations can use domain specific optimizations, or tiling and loop reordering to relieve the memory pressure.

In fact, in our experience the generated code is close to what users can, or already are, writing by hand, and vectorized parallel-for loop becomes just another abstraction for expressing high level computation. This further supports the need for subsequent optimizations.

Next we argue that $\hat{\gamma}(n)$ is functionally equivalent to SIMD execution of Γ . To establish equivalence, we need to show that given any valid execution ordering of nodes in $\hat{\gamma}(n)$, there is an execution ordering of nodes in $\gamma(i)$ whose SIMD execution produces the same output, and vice versa. We provide a sketch below. A formal proof, and dealing with stateful nested control flow will be left as out of scope of this paper.

First consider an execution ordering of $\gamma(i)$. A valid execution order in $\hat{\gamma}(n)$ can be constructed by mapping each node η to some valid execution ordering of nodes in $\hat{\eta}$. To see why this is a valid execution order of $\hat{\gamma}(n)$, first note that given our greedy conversion, there is an isomorphism between $\gamma(i)$ and $\hat{\gamma}(n)$ which maps each node η in the former to the sub-graph $\hat{\eta}$ in the latter. Secondly, functional equivalence of η and $\hat{\eta}$ follows from the correctness requirement of the converter for op_η . Thus, the given ordering in $\hat{\gamma}(n)$ simulates the SIMD execution of $\gamma(i)$.

Next consider the reverse direction, i.e. we are given an execution ordering in $\hat{\gamma}(n)$. We can similarly map each sub-graph $\hat{\eta}$ to a node η in $\gamma(i)$, but there are some tricky bits here. Firstly execution of $\hat{\eta}$ could be interleaved with execution of other nodes in $\hat{\gamma}(n)$. This is due to the non-determinism inherent in dataflow execution where it can run ready nodes in any order and even concurrently. Secondly, there could be multiple operations in $\hat{\eta}$ that touch mutable state at different times and we need to make sure η sees the same value for the state. To get an execution ordering, we first define a value $T_{\hat{\eta}}$ as follows. If $\hat{\eta}$ is stateless $T_{\hat{\eta}}$ is the time when the last input (including control dependency edges) to $\hat{\eta}$ got ready. For the case $\hat{\eta}$ accesses some state, we define $T_{\hat{\eta}}$ as the time the first read/write of some state actually happened inside $\hat{\eta}$. An equivalent execution ordering of $\gamma(i)$ can now be created by replacing $\hat{\eta}$ with η and ordering this sequence by $T_{\hat{\eta}}$.

To see why this ordering works, we first show that it is a valid execution order for $\gamma(i)$. If $T_{\hat{\eta}_1} < T_{\hat{\eta}_2}$, data or control dependencies from $\hat{\eta}_2$ to $\hat{\eta}_1$ are ruled out since all outputs of $\hat{\eta}_2$ are produced after $T_{\hat{\eta}_2}$ while all inputs of $\hat{\eta}_1$ are ready before $T_{\hat{\eta}_1}$ (see §3.8). Given our isomorphism, this similarly means that dependency from η_2 to η_1 is ruled out, thus ensuring validity of execution order. Next we argue why this ordering of nodes η simulates the execution of $\hat{\gamma}(n)$. To see that, note that accesses to state inside $\hat{\eta}$ are atomically done and in the order defined by $T_{\hat{\eta}}$. Ordering η in the same order thus allows us to enforce that the state evolves in the same way in Γ .

4 IMPLEMENTATION

Using the ideas mentioned in §3, we have implemented vectorization support in TensorFlow. We had the option of implementing this as an optimizing rewrite in the TensorFlow C++ runtime. However we chose to keep this in the Python frontend, as detailed below. This allowed us to build this external to TensorFlow and independent of the framework internals. In addition, for simplicity we chose to directly expose a `parfor` abstraction to the user instead of transparently optimizing sequential loops.

We provide a new Python function, `pfor`, with the following signature: `pfor(loop_body_fn, iters)`. Here `loop_body_fn` is a Python function that takes a scalar integer tensor, representing the loop variable, as input, and returns a nested structure of tensors. `iters` is a scalar integer tensor representing the number of `pfor` iterations to run. On being called, `pfor` returns a new set of graph nodes whose semantics is to runs the dataflow graph represented by `loop_body_fn` `iters` times, passing the values $0, 1, \dots, iters - 1$ to the different iterations, and stacking the outputs returned by these iterations. Here is an example.

```
a = tf.random_uniform([10, 20])
b = tf.random_uniform([10, 20])

def body(i):
    a_i = tf.gather(a, i)
    b_i = tf.gather(b, i)
    return a_i + b_i, a_i - b_i

# Equivalent to a + b, a - b
output = pfor(body, 10)
```

Here `body` returns two tensors with shape `[20]` that respectively represent the sum and the difference of the i^{th} rows of `a` and `b`. The semantics of this code is to run this function 10 times, passing values $0, \dots, 9$ and then stacking the outputs, returning two tensors, each with shape `[10, 20]`. Given our vectorization process, the call to `pfor` above returns tensors `a + b` and `a - b`.

Internally, the way it works is that the call to `pfor` first makes a single call to the function `body` to create a graph with four nodes (two `Gather`, one `Addition`, one `Subtraction`). Next the compiler is invoked which walks this graph using the greedy procedure describer earlier, and calls the converters for each node in the graph. Here the converters for `Gather` will return `a` and `b` respectively, since the vectorization process will essentially invert gathering each row. Next, converter for `Addition` will return `a + b` since that is the vectorization of adding the corresponding rows of its inputs. Similarly for `Subtraction`. Finally `pfor` will return these two symbolic tensors.

Most of our work has focused on cases where the shapes

of all inputs and outputs are loop invariant, and we have implemented support for more than 100 TensorFlow kernels, allowing us to vectorize models like convolutional networks and dynamic LSTMs. Shape invariance assumption allows us to use the vectorization layout we described in §3.4, which stacks all the underlying values along the first dimension.

We have also built some initial prototypes that handle shape variance, by padding the inputs to maximum shape and keeping track of the actual shapes of the underlying components. In initial experiments with networks involving convolutions, relu and dense layers on top of inputs with ragged shapes, we were able to generate code that closely matched the performance of hand written code.

5 APPLICATIONS

5.1 Jacobians

TensorFlow doesn't provide native support for computing jacobians efficiently. Instead it implements jacobian-vector products. It is easy to see that jacobian computation is essentially a parallel-for, where each iteration computes the gradient of one scalar value in the output tensor. However implementing this using a `tf.while_loop` is slow and doesn't always work. In particular, TensorFlow's `tf.while_loop` gradient computation involves popping tensors out of a TensorFlow stack data structure which is populated during the forward pass. This means that these gradient computations cannot be repeated multiple times as the stack will already be empty after the first gradient call is finished. Given this, jacobian computation of `tf.while_loop` (and in turn, `tf.nn.dynamic_rnn`) is not supported by TensorFlow. For the same reason, hessians (jacobian of jacobian) of non-scalar outputs doesn't work since that will involve jacobian of a `tf.while_loop` generated by the first jacobian call.

We provide a `jacobian` function, implemented using `pfor`, that is much faster than an iterative approach (§6.4). Given deep learning experiments can run for hours to days, these speedups alone make new research feasible. In addition, it enables the cases mentioned above, i.e., jacobians of `tf.while_loop` and `tf.nn.dynamic_rnn`, as well as hessians of non-scalar outputs.

Our support for jacobian has already been used by multiple researchers. For example, (Pfau et al., 2018) build upon efficient jacobian computation to create a framework for computing eigenfunctions of linear operators via stochastic optimization, and use it for unsupervised feature generation on video data. (Matt Golub, 2018) use our implementation to build a framework for finding and analyzing the fixed points of RNNs.

5.2 Auto-Batching

With auto-batching, users write their model code with a batch size of one, and then run that code across different inputs in a batch. The auto-batching framework makes it run faster by fusing similar operations. See §2 for a comparison of static and dynamic batching approaches and §6.2 for benchmarks.

Auto-batching can be implemented by invoking the forward pass (or some part) of the model in a `pfor` loop. Here is some example code.

```
def body(i):
    image, label = input_fn()
    prediction = model_fn(image)
    loss = loss_fn(prediction, label)
    return loss
```

```
losses = pfor(body, batch_size)
optimizer.minimize(losses)
```

As mentioned earlier in §4, most of our current implementation assumes shape invariance, but we have some initial results generating code that automatically pads and un pads ragged tensors. This can enable auto-batching popular networks, like *Transformers* (Dehghani et al., 2018). A harder case is efficient auto-batching of tree and graph traversals and tree RNNs (e.g. (Gilmer et al., 2017; Tai et al., 2015)), where padding may not be very efficient. On top of that, TensorFlow’s support for recursive data structures and functions is somewhat limited which may require resorting to iterative traversals and specialized representations. Getting a good trade-off of user experience and performance with such models is an open research problem.

5.3 Per-Example Gradients

The per-example gradients are regular gradients of the loss with respect to the variables, but the contributions from different examples in a batch are kept separate, not summed. Per-example gradients allow more sophisticated optimization strategies (e.g. (Alain et al., 2015)), but TensorFlow users today either need to run at batch size of 1, or perform special surgery on the generated graphs to compute per-example gradients. ((Goodfellow, 2015)).

Computing per-example gradients can be seen as a special case of auto-batching where one puts the gradient computation inside the `pfor` loop as well, and provides a cleaner and more efficient method for the same. Extending the example from §5.2

```
def body(i):
    image, label = input_fn()
    prediction = model_fn(image)
    loss = loss_fn(prediction, label)
```

```
return gradients(loss)
```

```
per_eg_grads = pfor(body, batch_size)
```

§6.3 shares some benchmark numbers for computing per-example gradients.

5.4 Optimizing Map Functions And Input Pipelines

`tf.map_fn` runs a given function, `fn`, over all row slices of a tensor, or a set of tensors, and stitches back the generated outputs. This can be directly implemented using `pfor`. Here is a sample implementation for the simple case of a single tensor input.

```
def pfor_map_fn(f, x):
    return pfor(
        lambda i: f(tf.gather(x, i)),
        tf.shape(x)[0])
```

Similarly `tf.data.Dataset` based pipelines provide a map function that transforms each of the elements of the Dataset. This is generally followed later by a call to `batch`. These calls can be swapped and the function passed to `map` can then be vectorized using the given batch size.

We benchmarked some toy input pipelines and simple `map_fn` calls. Using `pfor` sped these up one to two orders of magnitude, in-line with results seen in §6.

6 BENCHMARKS

6.1 Setup

Experiments were run on a 6 core Intel Xeon E5-1650 3.60GHz CPU with 64GB of RAM and a NVIDIA Maxwell Titan X GPU. We used two models in multiple experiments below. MNIST’s architecture is described in (tensorflow, 2016). It is a stack of two conv-relu-maxpool blocks followed by a linear-relu-dropout-linear block. Inputs are batches of 28×28 images and output has shape [10]. The LSTM model we used is a single-layer unidirectional RNN based on the LSTM cell described in (Hochreiter & Schmidhuber, 1997). Inputs are sequences of 128 dimensional vectors. LSTM state size is 256 except if mentioned otherwise (e.g. in §6.4).

6.2 Auto Batching

We compare the inference performance of 3 models implemented in different 4 way: using `pfor` auto-batching, using `tf.while_loop` to loop over inputs in a batch, and using DyNet with and without auto-batching enabled. Experiments are run with and without GPU support and reported in Figure 1. Throughput (measured as gigaflops or images/-tokens per second) is reported as function of batch size.

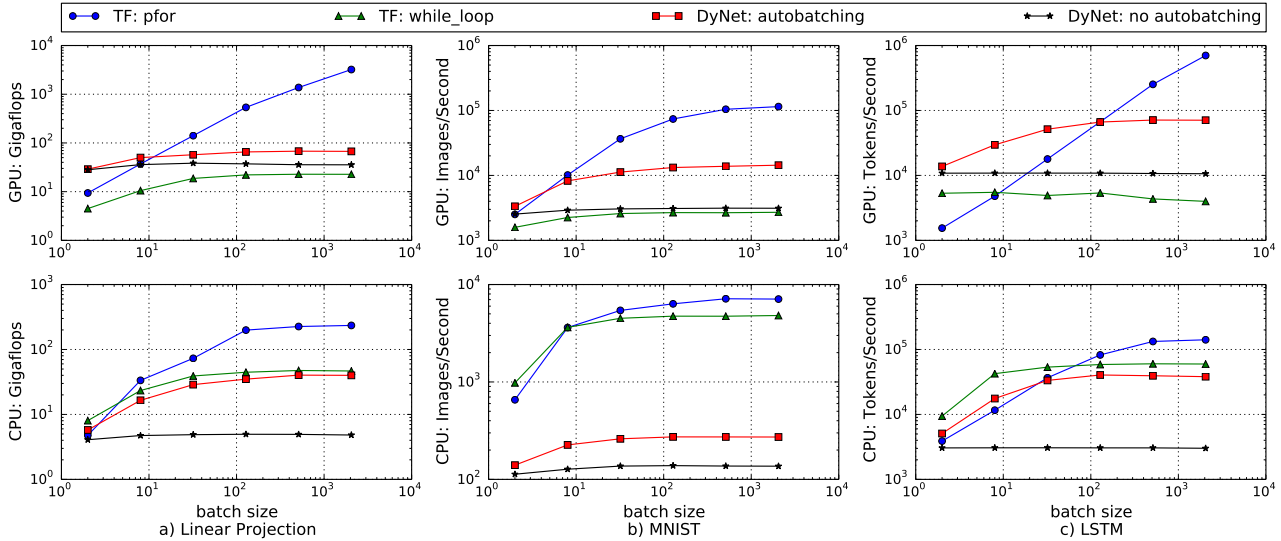


Figure 1. Auto-batching 3 models using DyNet and TensorFlow on GPU and CPU. Each column shows performance of a different model. Top row shows performance on GPU and bottom row on CPU. The x-axis is the batch size, i.e. the number of input examples that are auto-batched (in `pfor` and DyNet with auto-batching) or iterated over (for `tf.while_loop` and DyNet without auto-batching). The y-axis is the achieved throughput.

6.2.1 Linear Projection

We first study applying linear projection on input data. Inputs are randomly generated 768-dimensional vectors of floats. Projection matrix is a constant 768×768 matrix of floats. Figure 1a reports throughput measured in Gflops against batch size.

We notice that DyNet performs better than TensorFlow at small batch sizes, especially on GPU. In this regime, the computation time is dominated by fixed overheads, which appear lower for DyNet. For moderate to large batch sizes, `pfor`-based implementation outperforms the other three, by 1 to 1.5 orders of magnitude. The DyNet auto-batching based implementation does not scale as well at higher batch sizes likely because the auto-batching is performed at runtime and its cost is proportional to the batch size.

`tf.while_loop` does well on CPU since it supports running multiple loop iterations in parallel, hence utilizing multiple CPU cores. In our implementation, DyNet without auto-batching is driven from a single Python thread and fails to utilize multiple CPU cores. It is likely possible to use multiple Python threads to achieve higher performance without auto-batching.

6.2.2 MNIST

Figure 1b reports the number of images processed by the MNIST model per second as we vary the batch size. Overall trends look similar to those of the linear projection benchmark in §6.2.1. One noticeable difference is that on CPU

`tf.while_loop`'s performance scales better than in the linear projection benchmark. This is likely because the MNIST model requires more computation per iteration and execution overheads become less significant compared to it. `pfor` still outperforms the other three for moderate and large batch sizes.

6.2.3 LSTM

Figure 1c reports tokens per second processed by an LSTM as we vary batch size. Input sequence lengths for LSTM are sampled uniformly at random between 1 and 100, inclusively. The LSTM is implemented by iterating to the actual length for each sequence. We neither perform padding of the inputs, nor do we iterate to the maximum sequence length in a batch.

Here `pfor` needs relatively larger batch sizes to outperform other implementations and the margins are narrower. This is likely caused by the following two factors. Firstly, our implementation of vectorizing `tf.while_loop` still has considerable overheads, which we are working on optimizing. Secondly, given that sequence lengths are randomly chosen, iterations of the sequential loop generated by `pfor` progressively operate on smaller batches. Smaller batch sizes have lower hardware utilization and also smaller speedup from vectorization compared to other strategies. The overall speedup is an expectation over the speedups at different batch sizes and hence lower than the speedup for linear and MNIST models, which have a fixed batch size throughout an experiment.

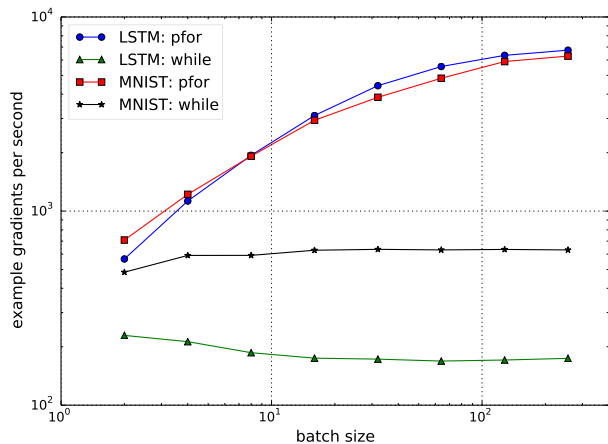


Figure 2. Throughput of per-example gradient computation on MNIST and LSTM with and without auto-vectorization, on GPU. The x-axis is the number of examples in the batch. The y-axis is the number of per-example gradients that can be computed.

6.3 Per-Example Gradients

In this benchmark we evaluate the number of example gradients that `pfor` and `tf.while_loop` based implementations can achieve versus the number of examples in the batch. Example is an image for MNIST and a complete input sequence for LSTM. All input sequences have length 10 in this benchmark. The `tf.while_loop` based implementation simply iterates over all the examples in the batch, computing gradients for each. `pfor` based implementation vectorizes this iteration.

Figure 2 shows that `tf.while_loop` based implementation achieves almost constant throughput for both MNIST and LSTM models. On the other hand, `pfor` based implementation is able to utilize the GPU better by vectorizing the gradient computation. At the highest batch size of 256 for the LSTM model, `pfor` outperforms `tf.while_loop` by a factor of 38.

6.4 Jacobians

This benchmark looks at computing jacobians of model output with respect to model inputs on GPU. As mentioned in 5.1, TensorFlow currently has no efficient native support for computing jacobians. The best available option is to compute the gradients of each scalar in the output with respect to inputs. Each such gradient is a row of the jacobian matrix. We vary the output size and measure throughput as rows of jacobian processed per second. This metric normalizes the compute done for a given task as we vary the output size. Figure 3 reports jacobian rows per second against output size.

Besides the LSTM model that we used in other bench-

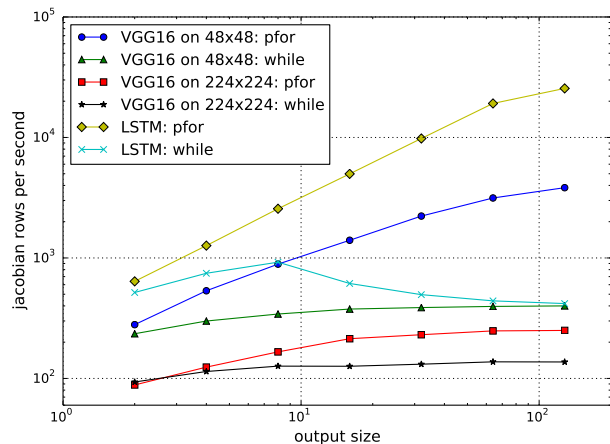


Figure 3. Throughput of computing jacobians (output with respect to input) for VGG16 and LSTM models as output size is varied, with and without vectorization, on GPU. VGG16 uses two different input image sizes.

marks, we picked the VGG16 (Simonyan & Zisserman, 2014) model since it supports different input image sizes as well as different number of output classes. We report results for two input image sizes: 48×48 and 224×224 . The LSTM model is statically unrolled to 10 steps in this benchmark because of the TensorFlow’s restriction described in §5.1.

Figure 3 shows that the unvectorized implementation scales poorly with output sizes. The only speed up it is able to get is from parallel execution of the loop body. `pfor` based implementation outperforms `tf.while_loop` based implementation by more than an order of magnitude at higher output sizes. At the largest output size of 128, `pfor` outperforms `tf.while_loop` by over 60x.

7 SUMMARY

We proposed applying static vectorization to dataflow IR like TensorFlow graphs. We implemented a library that provides vectorized parallel-for loop construct for TensorFlow. This enables applications ranging from static auto-batching and per-example gradients, to jacobians, Hessians and optimization of input pipelines. GPU benchmarks show speedups of up to two orders of magnitude compared to TensorFlow’s sequential loop and an order of magnitude against DyNet with dynamic batching. There is ongoing work on better handling loop variant shapes by automatic padding and masking.

Moving forward, these techniques can help optimize sequential loops. More research is needed in dealing with sparse computation, recursive computation like tree or graph traversals, handling memory constraints and applying polyhedral loop optimization, generating more optimized code using better heuristics and hardware cost models, etc.

REFERENCES

- Abadi, M., Agarwal, A., Barham, P., Brevdo, E., Chen, Z., Citro, C., Corrado, G. S., Davis, A., Dean, J., Devin, M., Ghemawat, S., Goodfellow, I. J., Harp, A., Irving, G., Isard, M., Jia, Y., Józefowicz, R., Kaiser, L., Kudlur, M., Levenberg, J., Mané, D., Monga, R., Moore, S., Murray, D. G., Olah, C., Schuster, M., Shlens, J., Steiner, B., Sutskever, I., Talwar, K., Tucker, P. A., Vanhoucke, V., Vasudevan, V., Viégas, F. B., Vinyals, O., Warden, P., Wattenberg, M., Wicke, M., Yu, Y., and Zheng, X. Tensorflow: Large-scale machine learning on heterogeneous distributed systems. *CoRR*, abs/1603.04467, 2016. URL <http://arxiv.org/abs/1603.04467>.
- Alain, G., Lamb, A., Sankar, C., Courville, A., and Bengio, Y. Variance Reduction in SGD by Distributed Importance Sampling. *ArXiv e-prints*, November 2015.
- Barik, R., Zhao, J., and Sarkar, V. Efficient selection of vector instructions using dynamic programming. In *Proceedings of the 2010 43rd Annual IEEE/ACM International Symposium on Microarchitecture*, MICRO '10, pp. 201–212, Washington, DC, USA, 2010. IEEE Computer Society. ISBN 978-0-7695-4299-7. doi: 10.1109/MICRO.2010.38. URL <https://doi.org/10.1109/MICRO.2010.38>.
- Chen, T., Moreau, T., Jiang, Z., Shen, H., Yan, E. Q., Wang, L., Hu, Y., Ceze, L., Guestrin, C., and Krishnamurthy, A. TVM: end-to-end optimization stack for deep learning. *CoRR*, abs/1802.04799, 2018. URL <http://arxiv.org/abs/1802.04799>.
- Dehghani, M., Gouws, S., Vinyals, O., Uszkoreit, J., and Kaiser, Ł. Universal Transformers. *ArXiv e-prints*, July 2018.
- Frostig, R., Johnson, M. J., and Leary, C. Compiling machine learning programs via high-level tracing. In *SysML*, 2018.
- Gers, F. A., Schmidhuber, J. A., and Cummins, F. A. Learning to forget: Continual prediction with lstm. *Neural Comput.*, 12(10):2451–2471, October 2000. ISSN 0899-7667. doi: 10.1162/089976600300015015. URL <http://dx.doi.org/10.1162/089976600300015015>.
- Gilmer, J., Schoenholz, S. S., Riley, P. F., Vinyals, O., and Dahl, G. E. Neural message passing for quantum chemistry. *CoRR*, abs/1704.01212, 2017. URL <http://arxiv.org/abs/1704.01212>.
- Goodfellow, I. Efficient Per-Example Gradient Computations. *ArXiv e-prints*, October 2015.
- Graves, A. Adaptive computation time for recurrent neural networks. *CoRR*, abs/1603.08983, 2016. URL <http://arxiv.org/abs/1603.08983>.
- Hochreiter, S. and Schmidhuber, J. Long short-term memory. *Neural Comput.*, 9(8):1735–1780, November 1997. ISSN 0899-7667. doi: 10.1162/neco.1997.9.8.1735. URL <http://dx.doi.org/10.1162/neco.1997.9.8.1735>.
- Karrenberg, R. and Hack, S. Whole-function vectorization. In *Proceedings of the 9th Annual IEEE/ACM International Symposium on Code Generation and Optimization*, CGO '11, pp. 141–150, Washington, DC, USA, 2011. IEEE Computer Society. ISBN 978-1-61284-356-8. URL <http://dl.acm.org/citation.cfm?id=2190025.2190061>.
- Looks, M., Herreshoff, M., Hutchins, D., and Norvig, P. Deep learning with dynamic computation graphs. *CoRR*, abs/1702.02181, 2017. URL <http://arxiv.org/abs/1702.02181>.
- Matt Golub. FixedPointFinder: a tensorflow toolbox for finding fixed points and linearized dynamics in recurrent neural networks. <https://github.com/mattgolub/fixed-point-finder>, 2018.
- Neubig, G., Goldberg, Y., and Dyer, C. On-the-fly operation batching in dynamic computation graphs. In Guyon, I., Luxburg, U. V., Bengio, S., Wallach, H., Fergus, R., Vishwanathan, S., and Garnett, R. (eds.), *Advances in Neural Information Processing Systems 30*, pp. 3971–3981. Curran Associates, Inc., 2017.
- Nuzman, D., Rosen, I., and Zaks, A. Auto-vectorization of interleaved data for simd. *SIGPLAN Not.*, 41(6):132–143, June 2006. ISSN 0362-1340. doi: 10.1145/1133255.1133997. URL <http://doi.acm.org/10.1145/1133255.1133997>.
- Paszke, A., Gross, S., Chintala, S., Chanan, G., Yang, E., DeVito, Z., Lin, Z., Desmaison, A., Antiga, L., and Lerer, A. Automatic differentiation in pytorch. 2017.
- Pfau, D., Petersen, S., Agarwal, A., Barrett, D., and Stachenfeld, K. Spectral Inference Networks: Unifying Spectral Methods With Deep Learning. *ArXiv e-prints*, June 2018.
- Pharr, M. and Mark, W. R. ispc: A spmd compiler for high-performance cpu programming. IEEE, 2012. ISBN 978-1-4673-2633-9. doi: 10.1109/InPar.2012.6339601. URL <https://ieeexplore.ieee.org/document/6339601>.
- Ragan-Kelley, J., Barnes, C., Adams, A., Paris, S., Durand, F., and Amarasinghe, S. Halide: A language and compiler for optimizing parallelism, locality, and recomputation in

- image processing pipelines. In *Proceedings of the 34th ACM SIGPLAN Conference on Programming Language Design and Implementation*, PLDI '13, pp. 519–530, New York, NY, USA, 2013. ACM. ISBN 978-1-4503-2014-6. doi: 10.1145/2491956.2462176. URL <http://doi.acm.org/10.1145/2491956.2462176>.
- Salesforce. Matchbox. <https://github.com/salesforce/matchbox>, 2018.
- Simonyan, K. and Zisserman, A. Very deep convolutional networks for large-scale image recognition. *CoRR*, abs/1409.1556, 2014. URL <http://arxiv.org/abs/1409.1556>.
- Tai, K. S., Socher, R., and Manning, C. D. Improved semantic representations from tree-structured long short-term memory networks. *CoRR*, abs/1503.00075, 2015. URL <http://arxiv.org/abs/1503.00075>.
- tensorflow. models/tutorials/image/mnist/convolutional.py. <https://github.com/tensorflow/models/blob/master/tutorials/image/mnist/convolutional.py>, 2016.
- The SciPy community. Broadcasting. <https://docs.scipy.org/doc/numpy/user/basics.broadcasting.html>, 2008.
- The XLA team. XLA - TensorFlow, compiled. <https://developers.googleblog.com/2017/03/xla-tensorflow-compiled.html>, 2017.
- Trifunovic, K., Nuzman, D., Cohen, A., Zaks, A., and Rosen, I. Polyhedral-model guided loop-nest auto-vectorization. In *Proceedings of the 2009 18th International Conference on Parallel Architectures and Compilation Techniques*, PACT '09, pp. 327–337, Washington, DC, USA, 2009. IEEE Computer Society. ISBN 978-0-7695-3771-9. doi: 10.1109/PACT.2009.18. URL <https://doi.org/10.1109/PACT.2009.18>.
- Wei, R., Adve, V., and Schwartz, L. DLVM: A modern compiler infrastructure for deep learning. *arXiv preprint arXiv:1711.03016*, 2017.
- Yu, Y., Abadi, M., Barham, P., Brevdo, E., Burrows, M., Davis, A., Dean, J., Ghemawat, S., Harley, T., Hawkins, P., Isard, M., Kudlur, M., Monga, R., Murray, D., and Zheng, X. Dynamic control flow in large-scale machine learning. In *Proceedings of the Thirteenth EuroSys Conference*, EuroSys '18, pp. 18:1–18:15, New York, NY, USA, 2018. ACM. ISBN 978-1-4503-5584-1. doi: 10.1145/3190508.3190551. URL <http://doi.acm.org/10.1145/3190508.3190551>.